to time. Temperatures during a given experimental run were then extrapolated from the calibration curve and the reading from the probe thermocouple. Temperature readings are accurate within 5 °C.[28]

Exchange rates were determined from the spectral line shape. Line shape analysis was done using the program DNMR-5 available through QCPE.

2-D NMR Exchange Rates. Sample Preparation. NMR samples were prepared by dissolving 3.5-4.1 mg of the diarylnaphthyl derivative in 0.5 mL of DMSO-d_6. Each sample contained 0.8 mM $Gd(NO_3)_3$. The gadolinium nitrate was used as a paramagnetic relaxation reagent to shorten the spin-lattice relaxation times of the methyl protons and decrease the time of the experiment.

NMR Spectroscopy. All spectra were recorded at 500 MHz and 143 °C (ethylene glycol standard).[29] Pure absorption two-dimensional exchange (2-D EXSY) spectra were recorded using the pulse sequence delay-90°-t_1-90°-τ_m-90°-t_2 and the method of phase cycling described by States et al.[30] with alternating block acquisition. The spectra were collected into 1024 data points in each block with quadrature detection using a spectral width of 1500 Hz and a mixing time of 300 ms. Typically, 512 t_1 experiments were collected and zero filled to 1 K. For each t_1 value, eight scans were signal averaged, with a recycle time of 3 s. A line broadening of 1 Hz was imposed in each dimension prior to Fourier transformation.

Determination of Rate Constants.[28] The volumes of the cross peaks and diagonal peaks of the 2-D data sets were evaluated by summing over all data points contained within a chosen peak integration radius. The rate constants for exchange were calculated by solving for **R** in eq 1,

$$I_{ij}(\tau_m) = M_j(o)(e^{-\mathbf{R}\tau_m})_{ij} \quad (1)$$

where I_{ij} is the integrated intensity of the two-dimensional absorption peak at mixing time τ_m, $M_j(o)$ is the equilibrium magnetization of the nuclei in site j, and **R** is a square matrix whose diagonal elements are $R_{ij} = T_{1,i-1} + \sum_l k_{il}$) and whose off-diagonal elements are $R_{ij} = -k_{jl}$.[31,32]

Acknowledgment. We thank the National Science Foundation Presidential Young Investigator Award Program (CHE-8857812), the American Cancer Society Junior Faculty Fellowship Program (C-58024), MURST-Roma, and the NATO Collaborative Research Grants Programme (RG. 0092/89). We greatly appreciate additional support of our program from the Exxon Educational Fund, Hofmann-La Roche, Rohm+Haas, Monsanto, Eli Lilly, and Sterling Drug. Funds for the 500-MHz NMR instrument were provided by the NIH (RR04733) and NSF (CHE8814866).

Registry No. I, 141397-24-2; II, 141397-25-3; III, 141397-26-4; IV, 14476-01-8; V, 141397-27-5; VI, 141397-28-6; VII, 141397-29-7; *syn*-VIII, 141435-25-8; *anti*-VIII, 141397-31-1; *syn*-IX, 141397-30-0; *anti*-IX, 141435-23-6; *syn*-X, 141435-24-7; *anti*-X, 141397-32-2; 4-methoxyiodobenzene, 696-62-8; 4-methyliodobenzene, 624-31-7; iodobenzene, 591-50-4; 4-chloroiodobenzene, 637-87-6; 4-(methoxycarbonyl)iodobenzene, 619-44-3; 4-nitrobenzene, 636-98-6; 1,8-dibromonaphthalene, 17135-74-9; 2-methyliodobenzene, 615-37-2; 2-methyl-4-methoxyiodobenzene, 63452-69-7; 2-methyl-4-chloroiodobenzene, 23399-70-4; 2-methyl-4-nitroiodobenzene, 5326-38-5.

(29) Kaplan, M. L.; Bovey, F. A.; Cheng, A. N. *Anal. Chem.* **1975**, *47*, 1703.
(30) States, D. J.; Haberkorn, R. A.; Ruben, D. J. *J. Magn. Reson.* **1982**, *48*, 286.
(31) Perrin, C. L.; Gipe, R. K. *J. Am. Chem. Soc.* **1984**, *106*, 4036.
(32) Dwyer, T. J. Ph.D. Thesis, University of California at San Diego, 1988.

Infrared Multiple Photon Studies of Alkoxide-Alcohol Complexes

Susan Baer[†] and John I. Brauman*

Contribution from the Department of Chemistry, Stanford University, Stanford, California 94305-5080. *Received December 17, 1990*

Abstract: Alkoxide-alcohol complexes, $R'OH{\cdot}RO^-$, were synthesized by an ion-molecule reaction in a Fourier transform ion cyclotron resonance mass spectrometer. Isotope labeling was used to differentiate between the two possible complexes: $ROH{\cdot}R'O^-$ and $R'OH{\cdot}RO^-$. The structure of the complexes was probed using infrared multiple photon dissociation. The ratio of the photoproducts ($RO^-/R'O^-$) was found to depend on the method of synthesis of the complex. This differentiation suggests that the two complexes are distinct; i.e., they retain some memory of their original identity. These results are not consistent with the simple hydrogen-bonded structure, which should have a very low barrier to proton transfer. The possibility of an isomeric structure which does not lie along the minimum energy path for proton transfer is discussed.

Introduction

Simple proton-transfer reactions between alkoxide ions with localized charge are not expected to have large energetic barriers. In solution, the majority of exothermic proton-transfer reactions between nonconjugated ions occur at the diffusion limit.[1] The gas-phase reactivity of alkoxide ions is not expected to differ significantly from that in solution. Indeed, quantum calculations of the gas-phase proton-transfer potential energy surface suggest that it is relatively smooth, with a proton-transfer barrier of less than 1 kcal/mol separating two strongly bound alcohol-alkoxide complexes.[2,3] This result is substantiated by fractionation factor measurements of methoxide-methanol and ethoxide-ethanol dimers,[3-5] which are consistent with a small proton-transfer barrier.

In another paper, we reported the surprising result that proton-transfer reaction efficiencies of alkoxides with alcohols are slower than expected.[6a] Thermoneutral proton transfers between methoxide and methanol, ethoxide and ethanol, and *tert*-butoxide and *tert*-butyl alcohol all displayed reaction efficiencies of ca. 30%,

[†]Current address: Department of Chemistry, University of British Columbia, Vancouver, BC, Canada V6T 1Y6.

(1) (a) Crooks, J. E. In *Proton Transfer Reactions*; Caldin, E. F., Gold, V., Eds.; Wiley and Sons: New York, 1975; Chapter 6. (b) Caldin, E. F. *Fast Reactions in Solution*; Wiley and Sons: New York, 1964; Chapters 1, 12. (c) Bell, R. P. *The Proton in Chemistry*; Cornell University Press: Ithaca, NY, 1959.
(2) (a) Roos, B. O.; Kraemer, W. P.; Diercksen, G. H. F. *Theor. Chim. Acta* **1976**, *42*, 77. (b) Scheiner, S.; Szczesniak, M. M.; Bigham, L. D. *Int. J. Quantum Chem.* **1983**, *23*, 739. (c) Szczesniak, M. M.; Scheiner, S. *J. Chem. Phys.* **1982**, *77*, 4586. (d) Scheiner, S. *Acc. Chem. Res.* **1985**, *18*, 174. (e) Scheiner, S.; Bigham, L. D. *J. Chem. Phys.* **1985**, *82*, 3316. (f) Scheiner, S. *J. Chem. Phys.* **1984**, *80*, 1982. (g) Hillenbrand, E. A.; Scheiner, S. *J. Am. Chem. Soc.* **1984**, *106*, 6266. (h) Scheiner, S. *J. Chem. Phys.* **1982**, *77*, 4039. (i) Scheiner, S. *J. Am. Chem. Soc.* **1981**, *103*, 315. (j) Gao, J.; Garner, D. S.; Jorgensen, W. L. *J. Am. Chem. Soc.* **1986**, *108*, 4784. (k) Jorgensen, W. L.; Ibrahim, M. *J. Comput. Chem.* **1981**, *2*, 7. (l) Busch, J. H.; de la Vega, J. R. *J. Am. Chem. Soc.* **1977**, *99*, 2397. (m) de la Vega, J. R. *Acc. Chem. Res.* **1982**, *15*, 185. Wolfe, S.; Hoz, S.; Kim, C.-K.; Yang, K. *J. Am. Chem. Soc.* **1990**, *112*, 4186.
(3) Weil, D. A.; Dixon, D. A. *J. Am. Chem. Soc.* **1985**, *107*, 6859.

0002-7863/92/1514-5733$03.00/0

well below the 50% efficiency expected for a barrierless or nearly barrierless thermoneutral proton-transfer reaction. In addition, exothermic proton-transfer reactions were also found to be slow, with even quite exothermic reactions displaying less than unit reaction efficiency. Statistical (RRKM) modeling of these measured reaction efficiencies suggested large energy barriers for the proton transfer within the ion–molecule complex, even for thermoneutral reactions. The behavior of the exothermic proton-transfer reactions could also be rationalized by large "intrinsic" activation energies, as predicted by Marcus theory.[8] Such large activation barriers are obviously inconsistent with the reaction surface derived from quantum calculations. Trajectory calculations,[6b] however, suggest that it is possible to have reactions which are slower than encounter controlled even on a barrierless surface. Consequently, the simple RRKM procedure used for "conventional" double minimum surfaces is not appropriate for characterizing these reactions.

In an attempt to understand the proton-transfer reaction potential surface better, we undertook the present study of alcohol–alkoxide complexes which we *assumed* would be the hydrogen-bonded alcohol–alkoxide intermediates in proton-transfer reactions. These complexes are known to be strongly bound; the stabilization energy for the methoxide–methanol complex has been measured to be 29.3 kcal/mol.[9] Its calculated optimum geometry is reported to be slightly asymmetric, with the proton more tightly bound to one of the alkoxide moieties.[2j-n,3] As noted, however, quantum calculations suggest that the energetic barrier between the two reaction complexes is small.

This calculated surface is consistent with the observed chemical reactivity of the alcohol–alkoxide complexes. The complexes have been observed to undergo exchange reactions with alcohols in a nondiscriminant manner; i.e., the distinction between the alkoxide and the alcohol is lost in the course of the exchange reaction.[10] This same type of nondiscriminant behavior has also been observed in transesterification reactions of the alcohol–alkoxide dimers, even when the acidity difference between the alcoholic moieties is large (up to 6 kcal/mol).[11]

In the present study, we use a photochemical technique, infrared multiple photon dissociation (IRMPD),[12] to probe the structure[13] of the complex $ROHOR^-$ formed by reaction of RO^- + HCOOR (the Riveros reaction), in an attempt to determine whether the complex is asymmetric and, if so, whether conversion between the two forms is facile. The alkoxide–alcohol dimers were synthesized asymmetrically, using isotope labeling to differentiate between the two possible intermediates, $RO^-\cdot HOR'$ and $ROH\cdot^-OR'$. Surprisingly, their photoproduct ratios, determined by IRMPD of the complexes, were found to depend on their mode of formation. This differentiation suggests that alcohol–alkoxide complexes *formed in this manner* are distinct from each other; i.e. they retain some memory of their original identity. Although this result may be connected with the slow observed proton-transfer reaction rates, the existence of a large energy barrier for simple proton transfer in the hydrogen-bonded $ROH\cdot^-OR$ complex is precluded by the results of quantum calculations. The results reported here can be rationalized if another intermediate is formed by the Riveros reaction. This intermediate would be an isomer of the expected hydrogen-bonded species and could be relatively nonreactive to proton transfer. Interestingly, this hypothesis could also explain anomalous methoxide–methanol binding energies extracted from electron photodetachment studies (see later).

Experimental Section

Chemicals. All chemicals were purchased from Aldrich and used as received, with the exception of the compounds mentioned below. Samples were degassed using three successive freeze–pump–thaw cycles prior to introduction to the high-vacuum system. Deuterated compounds, CD_3OH and CD_3CH_2OH, were purchased from MSD Isotopes, as was $^{13}CH_3OH$. Isotopically labeled formates, $HCOO^{13}CH_3$, $HCOOCD_3$, and $HCOOCH_2CD_3$, were synthesized from their respective alcohols using the method of Stevens and van Es[14] and isolated using preparative gas chromatography. Methyl and ethyl nitrite were synthesized in situ by reaction of isoamyl nitrite and the appropriate alcohol.[15] Dimethyl peroxide was prepared using an adaptation of a literature recipe.[16]

Experimental System. All experiments were carried out using Fourier transform ion cyclotron resonance spectrometry (FT-ICR), which has been described in detail elsewhere.[17] Experiments were performed with an IonSpec FTMS2000 mass spectrometer attached to a Varian vacuum system, extensively adapted over years of use. Ions were trapped in a 1-in. cubic cell, placed between the poles of an electromagnet, which was operated at 1.0–1.2 T. Typical background pressures were 0.5–2.0 × 10^{-8} Torr. Neutral gas pressures were measured using a Varian 844 vacuum ionization gauge and were uncorrected.

Alcohol–alkoxide complexes were synthesized in the ICR cell by reaction of the alkoxide with the corresponding alkyl formate, a well-known ion–molecule reaction,[10] eq 1. Alkoxide ions, with the exception of

$$RO^- + HCOOR' \rightarrow [ROH\cdots COOR']^- \rightarrow ROH\cdot^-OR' + CO \quad (1)$$

R, R′ = $^{12}CH_3$,$^{13}CH_3$; $^{13}CH_3$,$^{12}CH_3$; CH_3,CD_3; CD_3,CH_3; CH_3CH_2,CD_3CH_2; CD_3CH_2,CH_3CH_2

CH_3O^-, were generated by electron impact on the corresponding alkyl nitrites, which also produces a small amount of HNO^- (m/z = 31). Mass 31 was therefore ejected from the cell prior to photodissociation. Methoxide ion, CH_3O^-, was generated by electron impact on dimethyl peroxide to avoid confusion with HNO^-. Once formed, the alkoxide–alcohol complexes were isolated using standard notched ejection techniques. Typical neutral gas pressures used were alkyl nitrites or dimethyl peroxide, 1.5–2.5 × 10^{-7} Torr, and alkyl formates, 0.8–1.5 × 10^{-6} Torr.

Lasers. Two different infrared lasers were used to photodissociate the alcohol–alkoxide complexes: a pulsed Lumonics TEA 103-2 CO_2 laser and a home-built continuous wave (CW) CO_2 laser. The laser outputs were collimated with a gold plated copper spherical mirror (radius of curvature 10 m), directed into the ICR cell, reflected off a mirror at the back of the cell, and sent back collinearly out of the cell to a beam stop. Thus, the ions were exposed to fluences and intensities twice those of the incident beam.

For the pulsed laser, duty cycles of 1–2 s were used to accommodate the recharging time of the laser. A variable-delay TTL pulse was used to trigger the laser. Pulse length was ca. 4 μs, with approximately 50%

(4) (a) Ellenberger, M. R.; Farneth, W. E., Dixon, D. A. *J. Phys. Chem.* **1981**, *85*, 4. (b) Szulejko, J. E.; Wilkinson, F. E.; McMahon, T. B. Presented at the 37th ASMS Conference on Mass Spectrometry and Allied Topics, May 1989. (c) Gold, V.; Grist, S. *J. Chem. Soc. B* **1971**, 1665. (d) Kreevoy, M. M.; Liang, T. M. *J. Am. Chem. Soc.* **1980**, *102*, 3315.

(5) Barlow, S. E.; Dang, T. T.; Bierbaum, V. *J. Am. Chem. Soc.* **1990**, *112*, 6832.

(6) (a) Dodd, J.; Baer, S.; Moylan, C. R.; Brauman, J. I. *J. Am. Chem. Soc.* **1991**, *113*, 5942. (b) Quasi-classical trajectory calculations on a simplified model proton-transfer surface suggest that the slow reactions may be associated with the presence of multiple transition states, which can occur even on a barrierless surface. These transition states, presumably associated with rotor locking, would not explain the kind of behavior seen in these IRMP experiments: Lim, K. F., Brauman, J. I. *J. Chem. Phys.* **1991**, *94*, 7164. Also: Lim, K. F.; Brauman, J. I. *Chem. Phys. Lett.* **1991**, *177*, 326.

(7) Grabowski, J. J.; DePuy, C. H.; Van Doren, J. M.; Bierbaum, V. M. *J. Am. Chem. Soc.* **1985**, *107*, 7384.

(8) (a) Cohen, A. O.; Marcus, R. A. *J. Phys. Chem.* **1968**, *72*, 4249. (b) Dodd, J. A.; Brauman, J. I. *J. Phys. Chem.* **1986**, *90*, 3559. (c) Dodd, J. A.; Brauman, J. I. *J. Am. Chem. Soc.* **1984**, *106*, 5356.

(9) (a) Paul, G. J. C.; Kebarle, P. *J. Phys. Chem.* **1990**, *94*, 5184. (b) Meot-Ner, M.; Sieck, L. W. *J. Phys. Chem.* **1986**, *90*, 6687. (c) Meot-Ner, M.; Sieck, L. W. *J. Am. Chem. Soc.* **1986**, *108*, 7525.

(10) Blair, L. K.; Isolani, P. C.; Riveros, J. M. *J. Am. Chem. Soc.* **1973**, *95*, 1057.

(11) Baer, S.; Stoutland, P. O.; Brauman, J. I. *J. Am. Chem. Soc.* **1989**, *111*, 4097.

(12) For an overview of this technique, see, for example: (a) Johnson, C. E.; Brauman, J. I. In *Techniques for the Study of Ion Molecule Reactions*, Farrar, J. M., Saunders, W. H., Jr., Eds.; John Wiley: New York, 1988; Chapter X. (b) Lupo, D. W.; Quack, M. *Chem. Rev.* **1987**, *87*, 181. (c) Ashfold, M. N. R.; Hancock, G. *Gas Kinetics and Energy Transfer*; The Chemical Society: London, 1981; Vol. 4. (d) Danen, W. C.; Jang, J. C. In *Laser-Induced Chemical Processes*; Steinfeld, J. I., Ed.; Plenum Press: New York, 1981.

(13) For previous applications of this technique to reaction intermediates, see: (a) Moylan, C. R.; Jasinski, J. M.; Brauman, J. I. *Chem. Phys. Lett.* **1983**, *98*, 1. (b) Moylan, C. R.; Jasinski, J. M.; Brauman, J. I. *Chem. Phys. Lett.* **1985**, *107*, 1534.

(14) Stevens, W.; van Es, A. *Rec. Chim. Pays Bas* **1964**, *83*, 1287.

(15) Caldwell, G.; Bartmess, J. E. *Org. Mass Spectrom.*, **1982**, *17*, 19.

(16) Hanst, P. L.; Calvert, J. G. *J. Phys. Chem.* **1959**, *63*, 104.

(17) For a recent review of this technique, see: Freiser, B. S. In *Techniques for the Study of Ion-Molecule Reactions* Farrar, J. M., Saunders, W. H., Jr., Eds.; John Wiley and Sons: New York, 1988; Chapter 3.

of the intensity within the first 500 ns. Removing the nitrogen component of the gas mixture shortened the pulse length, thus increasing the average intensity. Manipulation of the gas mixture ratios in this way varied the average intensity of the beam from 0.2 to 2 MW·cm^{-2}, which corresponds to a variation in the photon absorption rate of 2×10^6 to 2×10^7 s^{-1}, assuming an average photon absorption cross section of ca. 10^{-19} cm^2. Pulse fluence was controlled by passing the beam through CaF_2 attenuators; typically fluences were chosen to be 0.6–0.7 J·cm^{-2}. Two different laser lines were used: 9.6 μm (P20) and 10.6 μm (P22).

The CW laser, run at comparable average power to the pulsed laser, has, because of its continuous nature, much lower instantaneous power and lower intensity than the pulsed laser. Typical beam intensities were 15–18 W·cm^{-2}, corresponding to a photon absorption rate of ca. 1×10^2 s^{-1}, again assuming an average photon absorption cross section of ca. 10^{-19} cm^2. Because of this low power, no attenuation of either intensity or fluence was attempted. Irradiation times were controlled by triggering a mechanical shutter which prevented the CW beam from entering the ICR cell.

Experimental Procedure. In a typical experimental duty cycle using the pulsed laser, alkoxide ions were formed from the corresponding alkyl nitrite, or peroxide during the 20-ms electron beam pulse at the beginning of the duty cycle. Electrons were ejected during the following 20 ms. At the pressures used, alcohol–alkoxide complexes were completely formed, i.e., no more alkoxide ion remained in the cell, within ca. 100 ms. These complexes have been observed to undergo transesterification reactions with the neutral formates present in the ICR cell,[11] thus obscuring their identity and creating new isotopic species. For this reason, photodissociation was carried out as soon as a significant concentration of complex ions had developed, usually after 70–80 ms. Any remaining unsolvated alkoxide ions and small amounts of undesired labeled isotopic complexes (i.e., either unlabeled or doubly labeled species) were ejected from the cell using double-resonance techniques before the laser was fired, in order to avoid confusion with the photoproducts. The remaining alkoxide–alcohol population may be slightly contaminated by the reaction of small impurities of the undesired alkoxide with small impurities of the undesired alkyl formate. This isotopic species would have the same mass as the desired complex and therefore would not be ejected from the cell. This contamination is insignificant because of the small probability of reaction between two species both present in very small abundances. Furthermore, if these complexes were present, they would only diminish the synthesis differences which we observe experimentally. The photoproducts were detected 2–3 ms after irradiation by the appropriate laser. Mass balance of the photoproducts and reactants was observed with both the CW and pulsed lasers.

The amount of reactant photodissociation is directly dependent on the number of photons (fluence), i.e., the laser intensity multiplied by the time of irradiation. Because of the high fluence of the pulsed laser irradiation, almost total photodissociation of the alcohol–alkoxide complex was observed, despite the 4-μs pulse length. Photodissociation yields from CW laser photolysis are much lower for a given irradiation time, due to the lower average intensity of the beam. Total CW laser photodissociation could be observed after 125–150 ms of irradiation. However, due to the possibility of subsequent reactions of the photoproducts, the shortest possible CW laser irradiation time which produced a measurable amount of photoproducts was used. Irradiation times of 20–30 ms were typical, resulting in 10–20% photodissociation of the complex.

In order to ensure measurement of accurate photoproduct ratios, extensive averaging of each alcohol–alkoxide photodissociation was performed. In addition, small ion abundances were used in order to minimize the possibility of space charge effects arising from the presence of large amounts of ions in the cell. Experiments were performed on several different days to minimize any possible error. The actual photoproduct ratios obtained for each experiment are given in Table VI (see Appendix).

Results

The complexes for three different alkoxide + alcohol reactions were studied: $^{12}CH_3O^-$ + $^{13}CH_3OH$; CH_3O^- + CD_3OH; and $CH_3CH_2O^-$ + CD_3CH_2OH. In each case, the complex was generated in two different ways, eq 1, starting with the isotopically labeled alkoxide or starting with the isotopically labeled formate. In this way, six potentially different complexes were studied. Each complex was probed with the pulsed CO_2 laser and with the CW CO_2 laser. In each case, the only photoproducts observed were the labeled or unlabeled alkoxide moieties of the reaction complex. Two different pulsed laser lines were used: 9.6 μm (P20) and 10.6 μm (P22). No wavelength dependence of the photoproduct ratios was observed. The averaged ratios of labeled versus unlabeled photoproducts obtained for each complex with the pulsed and CW lasers are shown in Table I.

Table I. Average Photoproduct Ratios (Unlabeled/Labeled Alkoxides) Obtained from IRMPD of Alkoxide–Alcohol Complexes

$$RO^- + HCOOR' \rightarrow ROH{\cdot}{}^-OR'$$

complex (R, R′)	pulsed laser[a] irradiatn	CW laser[a] irradiatn
$^{13}CH_3$, $^{12}CH_3$	1.46 ± 0.12	1.0 ± 0.1
$^{12}CH_3$, $^{13}CH_3$	0.73 ± 0.16	1.0 ± 0.1
CD_3, CH_3	4.5 ± 0.8	5.1 ± 1.0
CH_3, CD_3	2.0 ± 0.2	4.5 ± 1.0
CD_3CH_2, CH_3CH_2	2.5 ± 0.4	2.6 ± 0.4
CH_3CH_2, CD_3CH_2	1.1 ± 0.2	2.1 ± 0.8

[a] All photoproduct ratios are of the form unlabeled alkoxide/labeled alkoxide.

Energetics. The reaction enthalpies of the corresponding proton-transfer reactions are not exactly zero, due to the effect of isotopic substitution on the molecule's zero point energy.[18] This effect is minimal, however, for ^{13}C substitution, and thus the proton-transfer reaction of [^{13}C]methoxide with [^{12}C]methanol, corresponding to complexes **1a** and **1b**, is essentially thermoneutral. Deuterium substitution has a much larger effect on the zero point energy. The reaction of deuterated methoxide with methanol, corresponding to **2a** and **2b**, has been measured to be 0.5 kcal/mol exothermic.[5,19]

$^{13}CH_3OH{\cdot}{}^{12}CH_3O^-$ **1a** $\quad$ $^{12}CH_3OH{\cdot}{}^{13}CH_3O^-$ **1b**

$CD_3OH{\cdot}CH_3O^-$ **2a** $\quad$ $CH_3OH{\cdot}CD_3O^-$ **2b**

The reaction of $CD_3CH_2O^-$ with CH_3CH_2OH yielding CD_3CH_2OH and $CH_3CH_2O^-$, shown in eq 2, is estimated to be 0.05 kcal/mol exothermic using the following method. The enthalpy change, i.e., the difference in acidity between the labeled and unlabeled ethanol, was roughly approximated to arise solely from the change in the three β C–H stretching vibrations, ignoring the other smaller frequency changes in the other vibrational modes. The change in frequency between unsubstituted ethanol and ethoxide was derived from the calculated difference in bond length for the two species[20] and an empirical relationship between bond length and frequency (Badger's rule),[21] shown in eq 3, where r_e is the bond length, and k_0 is the bond stretching force constant.

$$CD_3CH_2O^- + CH_3CH_2OH \rightarrow CD_3CH_2OH + CH_3CH_2O^- \quad (2)$$

$$k_0(r_e - 0.335)^3 = 1.86 \times 10^5 \quad (3)$$

The frequencies of the deuterated ethanol and ethoxide were approximated using eq 4,

$$\nu_D/\nu_H = (\mu_H/\mu_D)^{1/2} = 0.734 \quad (4)$$

where ν_H and ν_D are the frequencies of the undeuterated and deuterated species, respectively, and μ_D and μ_H are the reduced masses of C–D and C–H, respectively.[22] With these frequencies for ethanol, deuterated ethanol, ethoxide, and deuterated ethoxide, the change in zero point energy (ΔZPE) and then the enthalpy

(18) (a) Wolfsberg, M. *Acc. Chem. Res.* **1972**, *5*, 225. (b) DeFrees, D. J.; Hassner, D. Z.; Hehre, W. J.; Peter, E. A.; Wolfsberg, M. *J. Am. Chem. Soc.* **1978**, *100*, 641. (c) DeFrees, D. J.; Taagepara, M.; Levi, B. A.; Pollack, S. K.; Summerhays, K. D.; Taft, R. W.; Wolfsberg, M.; Hehre, W. J. *J. Am. Chem. Soc.* **1979**, *101*, 5532. (d) Hout, R. F., Jr.; Wolfsberg, M.; Hehre, W. J. *J. Am. Chem. Soc.* **1980**, *102*, 3296. (e) Hout, R. F.; Jr.; Levi, B. A.; Hehre, W. J. *J. Comput. Chem.* **1983**, *4*, 499.
(19) DeFrees, D. J.; Bartmess, J. E.; Kim. J. K.; McIver, R. T., Jr.; Hehre, W. J. *J. Am. Chem. Soc.* **1977**, *99*, 6451.
(20) Wiberg, K. B. *J. Am. Chem. Soc.* **1990**, *112*, 3379.
(21) Badger, R. M. *J. Chem. Phys.* **1934**, *2*, 128.
(22) Herzberg, G. *Spectra of Diatomic Molecules*, 2nd ed.; Van Nostrand Reinhold: Toronto, 1950; p 141.

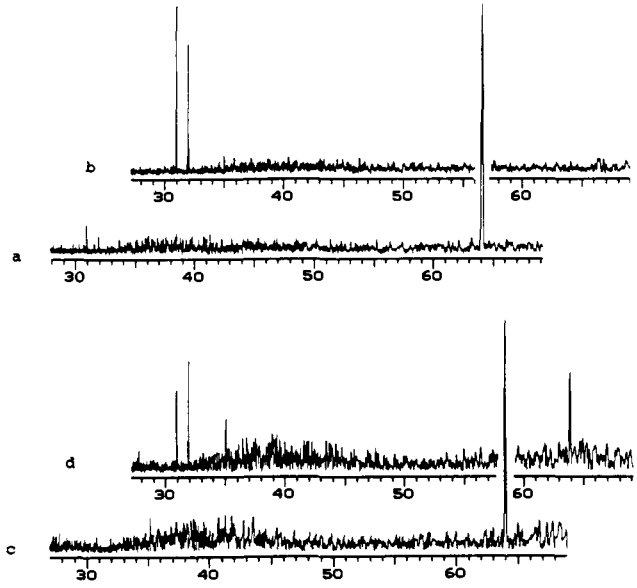

Figure 1. (a,b) Representative light-off and light-on mass spectra, respectively, of the methoxide–methanol complex formed by reaction of $^{13}CH_3O^-$ with $HCOO^{12}CH_3$. Before irradiation, the complex, at 64 amu, is the only ion present. After irradiation, both [^{12}C]methoxide (31 amu) and [^{13}C]methoxide (32 amu) are observed in approximately a 1.46/1 ratio. A noise peak (off scale in these figures) appears on both the mass spectra at a frequency corresponding to 70 amu at 10 kG, the magnetic field used for these experiments. (c,d) Representative light-off and light-on mass spectra, respectively, of the methoxide–methanol complex formed by reaction of $^{12}CH_3O^-$ with $HCOO^{13}CH_3$. Before irradiation, the complex, at 64 amu, is the only ion present. After irradiation, both [^{12}C]methoxide (31 amu) and [^{13}C]methoxide (32 amu) are observed in approximately a 0.76/1 ratio. A noise peak (off scale in these figures) appears on both the mass spectra at a frequency corresponding to 70 amu at 10 kG, the magnetic field used for these experiments. The small peak at 35 amu occurs at one-half that noise frequency.

change for the proton-transfer reaction ($\Delta H°_{rxn}$) can be calculated using eq 5 and 6, respectively. The average β C–H bond length

$$\Delta ZPE = 3(0.734)[\nu(C\text{–}H)_{EtOH} - \nu(C\text{–}H)_{EtO^-}] - 3[\nu(C\text{–}H)_{EtOH} - \nu(C\text{–}H)_{EtO^-}] \quad (5)$$

$$\Delta H°_{rxn} = \tfrac{1}{2}h\Delta ZPE \quad (6)$$

of ethanol[20] is 1.085 Å, and the average β C–H bond length of ethoxide[20] is 1.092 Å, which translates into a 55-cm^{-1} change in frequency between ethanol and ethoxide, using eq 3. Using this value, the change in zero point energy for eq 2 is calculated to be −44 cm^{-1} and $\Delta H°_{rxn}$ is calculated to be −0.05 kcal/mol.

In order to check the accuracy of this calculation, the acidity difference between CH_3OH and CD_3OH was also calculated using the method outlined above. The average C–H bond length of CH_3OH is 1.085 Å, and the C–H bond length of methoxide is 1.124 Å.[20] The calculated result was 0.43 kcal/mol, in rough agreement with the experimental value of 0.5 kcal/mol. The fact that this calculation underestimates the true acidity difference between methoxide and deuterated methoxide is not surprising since, as mentioned above, it considers only the vibrational mode most affected by deprotonation and ignores the other smaller changes in the vibrational frequencies. The much smaller acidity difference calculated for CH_3CH_2OH and CD_3CH_2OH (0.05 kcal/mol) than for CH_3OH and CD_3OH is expected since the deuteriums in the labeled ethanol are two bonds removed from the site of negative charge in the anion.

Photodissociation. Alcohol–alkoxide complexes **1a** and **1b** are both potential reaction intermediates in the thermoneutral proton exchange reaction of [^{12}C]methoxide with [^{13}C]methanol. Complex **1a** was produced by reaction of $^{13}CH_3O^-$ with $HCOO^{12}CH_3$. Complex **1b** was produced by reaction of $^{12}CH_3O^-$ with $HCOO^{13}CH_3$. Pulsed laser photodissociation of both complexes yielded the same photoproducts, $^{12}CH_3O^-$ and $^{13}CH_3O^-$, but in very different ratios, as shown in Table I. The $^{12}CH_3O^-/^{13}CH_3O^-$ ratio obtained for **1a** was 1.46/1. For **1b** the ratio was 0.73/1, roughly the inverse of the **1a** ratio. Complete photodissociation of the alcohol–alkoxide dimer using the pulsed CO_2 laser was usually observed in both complexes. Representative light-on and light-off mass spectra of **1a** and **1b** using pulsed laser irradiation are shown in Figure 1.

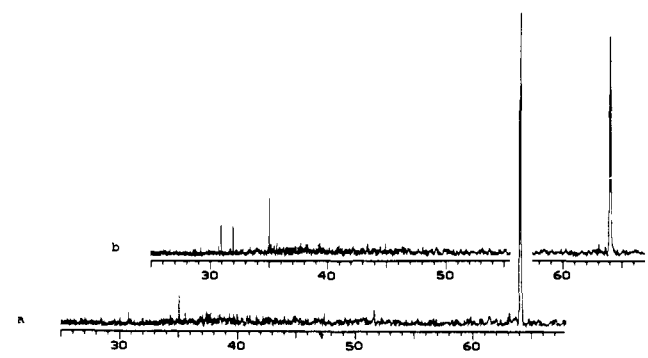

Figure 2. (a,b) Representative light-off and light-on mass spectra, respectively, of the methoxide–methanol complex formed by reaction of $^{13}CH_3O^-$ with $HCOO^{12}CH_3$. The irradiation in this case was for 15 ms, with a power of 20 W·cm^{-2} (twice the incident power at the cell). A noise peak (not shown) appears at a frequency corresponding to 70 amu at 10 kG; the peak at 35 amu occurs at one-half that noise frequency.

Table II. Input Parameters for RRKM Calculations of Methoxide + Methanol

reactant complex: $(CH_3O^-\cdot HOCH_3)$			orbiting transition state: $(CH_3O^-\cdots HOCH_3)$		
ν_i (cm^{-1})[a]		I_i (amu·Å), σ_i[b]	ν_i (cm^{-1})[a,c]		I_i (amu·Å), σ_i[b]
3681	1477		3681	1477	
3000	1455	21.27,[c] 1 (1)	3000	1455	28.90,[c] 1 (1)
3000	1455		3000	1455	1.83, 3 (1)
2960	1345		2960	1345	20.98, 1 (2)
2960	1165		2960	1165	18.66, 1 (2)
2844	1165		2844	1165	
2844	1060		2844	1060	
1477	1060		1477	1060	
1477	1033		1477	1033	
1477	1033		1477	1033	
300	250			250	
300	200				
300	200				
300					
$I_{reactant\ complex}$ = 193 amu·Å			$I_{transition\ state}$ = 606 amu·Å		

[a] Reference 31. Frequencies for CH_3O^- were taken from those of CH_3OH. [b] Degeneracy is in parentheses. [c] External rotation about the internuclear axis treated as an internal rotation able to exchange energy with other modes.

Photodissociation of **1a** and **1b** with the CW laser yielded equal amounts of $^{12}CH_3O^-$ and $^{13}CH_3O^-$, as shown in Table I. Only 10–20% photodissociation of either complex was observed. A representative result is shown in Figure 2. The photodissociation mass spectra of **1b** obtained with the CW laser were indistinguishable from those of **1a**.

Complexes **2a** and **2b**, potential intermediates in the CH_3O^- + CD_3O^- reaction, displayed similar behavior. Complex **2a** was formed by reaction of CD_3O^- with $HCOOCH_3$, while **2b** was formed by reaction of CH_3O^- with $HCOOCD_3$. Assuming that the energies of the complexes (which involve alkoxide ions) reflect the energies of the alkoxides themselves, complex **2a** is expected to be more stable than **2b** due to the 0.5 kcal/mol difference in acidities between CH_3OH and CD_3OH.[13,19] Results from photodissociation are shown in Table II. Pulsed laser photodissociation of the complexes yielded the two photoproducts, CH_3O^- and CD_3O^-, in different ratios. The unlabeled/labeled photoproduct ratio, CH_3O^-/CD_3O^-, for **2a** was 4.5/1 and for **2b** was 2.0/1. Thus, in this case, the more stable ionic photoproduct, CH_3O^-, always dominated, but proportionally less of it was generated from pulsed photodissociation of **2b** than **2a**. Representative light-on and light-off mass spectra for pulsed laser

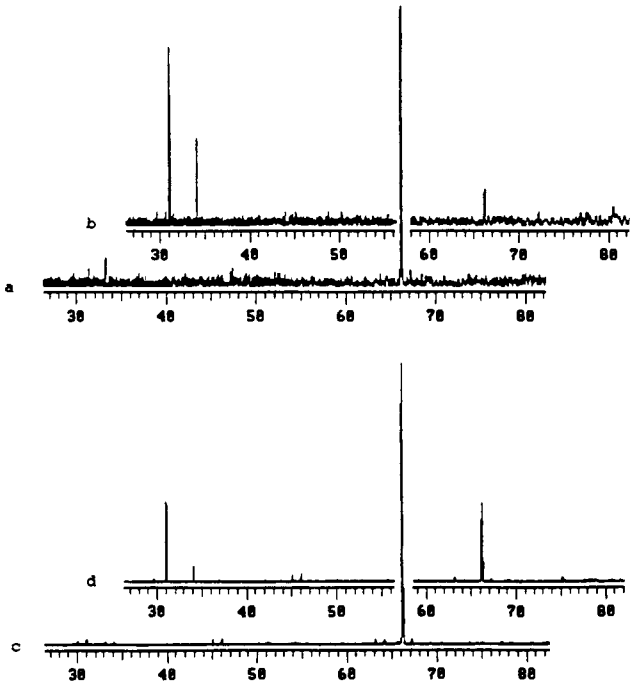

Figure 3. (a,b) Representative light-off and light-on mass spectra, respectively, of the methoxide–methanol complex formed by reaction of CH_3O^- with $HCOOCD_3$. Before irradiation, the complex, at 66 amu, is the only ion present. After irradiation, both methoxide (31 amu) and deuterated methoxide (34 amu) are observed in approximately a 2/1 ratio. (c,d) Representative light-off and light-on mass spectra, respectively, of the methoxide–methanol complex formed by reaction of CD_3O^- with $HCOOCH_3$. Before irradiation, the complex, at 66 amu, is the only ion present. After irradiation, both methoxide (31 amu) and deuterated methoxide (34 amu) are observed in approximately a 4.5/1 ratio.

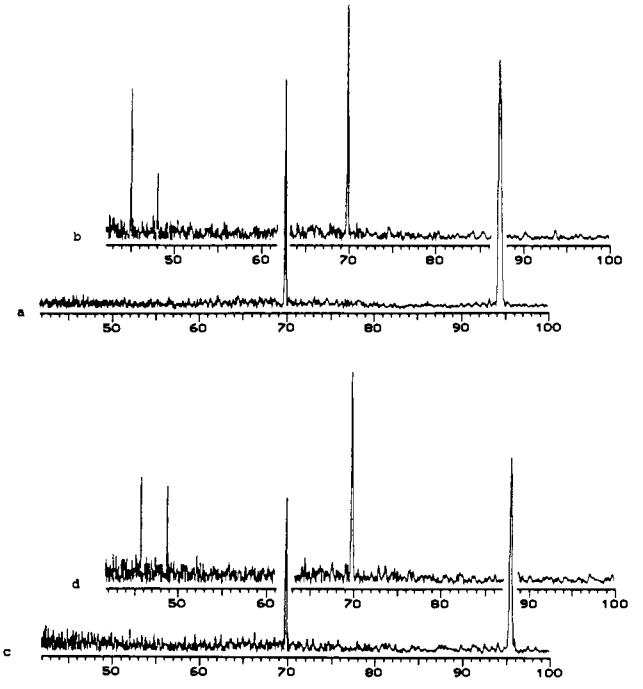

Figure 4. (a,b) Representative light-off and light-on mass spectra, respectively, of the ethoxide–ethanol complex formed by reaction of $CD_3CH_2O^-$ with $HCOOCH_2CH_3$. Before irradiation, the complex, at 94 amu, is the only ion present. After irradiation, both ethoxide (45 amu) and deuterated ethoxide (48 amu) are observed in approximately a 2.5/1 ratio. A noise peak appears on both the mass spectra at a frequency corresponding to 70 amu at 10 kG, the magnetic field used for these experiments. (c,d) Representative light-off and light-on mass spectra, respectively, of the ethoxide–ethanol complex formed by reaction of $CH_3CH_2O^-$ with $HCOOCH_2CD_3$. Before irradiation, the complex, at 94 amu, is the only ion present. After irradiation, both ethoxide (45 amu) and deuterated ethoxide (48 amu) are observed in approximately a 1.1/1 ratio. A noise peak appears on both the mass spectra at a frequency corresponding to 70 amu at 10 kG, the magnetic field used for these experiments.

photolysis of **2a** and **2b** are shown in Figure 3.

Photodissociation of **2a** using the CW CO_2 laser yielded a CH_3O^-/CD_3O^- ratio of 5.1/1, while photodissociation of **2b** yielded a CH_3O^-/CD_3O^- ratio of 4.5/1. Since these two values are equivalent within experimental error, the average CW dissociation ratio of both complexes was taken to be 4.8/1.

The potential intermediates in the reaction of $CH_3CH_2O^-$ with CD_3CH_2OH, complexes **3a** and **3b**, also displayed similar photochemical behavior. Complex **3a** was formed by reaction of $CD_3CH_2O^-$ with $HCOOCH_2CH_3$, while **3b** was formed by reaction of $CH_3CH_2O^-$ with $HCOOCH_2CD_3$. As in the case of the deuterated methanol system, **3a** is expected to be slightly energetically favored over **3b** due to the 0.05 kcal/mol estimated acidity difference between CD_3CH_2OH and CH_3CH_2OH. The photodissociation results are shown in Table I. Two photoproducts, $CH_3CH_2O^-$ and $CD_3CH_2O^-$, were observed from photodissociation of either complex with both the pulsed and CW lasers. Dissociation of **3a** with the pulsed laser yielded a $CH_3CH_2O^-/CD_3CH_2O^-$ ratio equal to 2.5, while the corresponding dissociation of **3b** yielded a $CH_3CH_2O^-/CD_3CH_2O^-$ ratio equal to 1/1. Thus, in the case of **3b**, almost equal amounts of the two photoproducts were observed, whereas dissociation of **3a** yielded significantly more of the unlabeled alkoxide. Representative light-on and light-off mass spectra for **3a** and **3b** using pulsed laser irradiation are shown in Figure 4.

$$\underset{\mathbf{3a}}{CD_3CH_2OH\cdot CH_3CH_2O^-} \qquad \underset{\mathbf{3b}}{CH_3CH_2OH\cdot CD_3CH_2O^-}$$

Photodissociation of **3a** with the CW CO_2 laser yielded an undeuterated to deuterated alkoxide ratio of 2.6/1, and dissociation of **3b** yielded a similar ratio of 2.1/1. Again, these ratios are equivalent within the limits of experimental error, and thus, the average CW dissociation ratio was taken to be 2.3/1.

Discussion

The photochemical behavior of the alkoxide–alcohol complexes, discussed above, is striking. The "same" reaction intermediate, differentiated synthetically only by switching the isotopic labeling in eq 1, yields different photoproduct ratios upon irradiation with the pulsed CO_2 laser. This differentiation implies that the alkoxide–alcohol complex formed by the Riveros reaction retains some memory of its original identity; i.e., within the lifetime of the complex, proton equilibration between the two alkoxide moieties is not achieved. This result suggests the existence of (at least) two distinct intermediates which lie somewhere on the proton-transfer reaction surface. While these intermediates may be associated with the observed slow reaction kinetics,[16] this is inconsistent with the proton-transfer reaction surface derived from quantum calculations. A more likely explanation is that the intermediates lie in local minima which are unrelated to the minimum energy proton-transfer reaction path.

Before discussing the photoproduct ratios measured in this paper, it is instructive to consider a phenomenological picture of the different processes involved in infrared multiple photon dissociation of the alcohol–alkoxide complexes formed by the Riveros reaction. (For the sake of simplicity in this qualitative description, the possible existence of multiple intermediates on the proton-transfer reaction surface is disregarded.) The product ratio obtained upon irradiation of the alkoxide–alcohol complex depends on a competition between four rates:[23] k_a, the photon absorption rate, which itself depends on the intensity of the laser beam; k_{-a}, the rate of stimulated emission; k_{-1}, the rate of decomposition of the reactive intermediate; and k_2, the rate of complex interconversion. During the laser pulse, the complex ion is pumped up the vibrational manifold, absorbing energy until k_{-1} or k_2 competes

(23) For the purposes of this discussion, the photon absorption rate, k_a, is assumed to be equal for all the alkoxide–alcohol complexes.

with k_a. If the barrier to proton transfer is small, as suggested by the quantum calculations for the hydrogen-bonded alcohol–alkoxide intermediates, the sum of states for the proton-transfer transition state and therefore the rate of proton transfer will be quite large before the dissociation, and no distinction between the isomeric complexes will be observed. If, on the other hand, the barrier to complex interconversion is substantial, the situation becomes more complicated. Although complex interconversion must have a lower threshold energy than decomposition, as energy increases, k_{-1} increases more quickly than k_2 due to a higher sum of states in the orbiting transition states than in the interconversion transition state. If k_a is large, k_{-1} and k_2 can compete successfully only at high energies. At these energies, k_{-1} is faster than k_2, and decomposition into reactants is the dominant process; photodissociation of the two isomeric species will therefore yield different photoproduct ratios. If on the other hand k_a is small, k_2 can compete with photon absorption at lower energies, leading to equilibration between the complexes before dissociation.

For this reason, when a barrier to complex interconversion exists, the photoproduct ratio is strongly dependent on the intensity of the laser beam. The CW laser, with its low intensity ($k_a \approx 10^2$ s^{-1}), is expected to yield only the lowest energy photoproduct; as soon as the dissociation threshold is reached, decomposition is faster than further photon absorption, and thus all decomposition occurs no more than 1 photon above threshold.[24] In the case of the alkoxide–alcohol complexes, this low photon absorption rate should lead to proton equilibration between the two complexes before the decomposition threshold is attained. The pulsed CO_2 laser has a much larger photon absorption rate, on the other hand ($k_a \approx 10^7$ s^{-1}), and thus the possibility of photoproduct branching exists.

Previous IRMPD studies by Moylan, Jasinski, and Brauman[13] have examined asymmetric alkoxide–alcohol complexes in which the acidity difference between the two alcohols is relatively large. Results from these studies and others[25] suggest that the thermodynamic product usually predominates, even with high-intensity irradiation, unless the energy difference between the two dissociation channels is extremely small, or an energetic or entropic barrier hampers dissociation to the thermodynamically favored channel. For example, in the case of *tert*-butoxide–methanol, where the acidity difference between methanol and *tert*-butyl alcohol is 6 kcal/mol,[26] pulsed laser photodissociation yielded only *tert*-butoxide, the energetically favored product. Branching is observed, however, in the pulsed laser dissociation of *tert*-butoxide–HF, where the two photoproducts, *tert*-butoxide and F^-, are almost equal in energy.[26] Branching has also been observed in the photodissociation of proton-bound alcohol dimer cations by Bomse and Beauchamp, using a low-power (<100 W/cm^2) CW laser.[27] Since this type of slow irradiation is expected to provide reaction via only the slowest channel, this result suggests that the three photoproduct channels observed, protonated alcohols, protonated ethers, and proton-bound alcohol–water dimers, must have the same threshold kinetics. (This does not necessarily imply that the photoproducts are equal in energy, since product branching could occur *after* a single photochemical step.)[25]

On the basis of these earlier studies, one would expect that infrared irradiation of the thermoneutral alkoxide–alcohol dimers, differentiated only by isotopic labeling, **1a** and **1b**, would yield equal amounts of the labeled and unlabeled alkoxide ions. Since the photoproducts, $^{12}CH_3O^-$ and $^{13}CH_3O^-$, are thermodynamically equivalent, both the CW and pulsed laser experiments should yield the same result. This behavior, however, is not observed. Complexes **1a** and **1b** yield different ratios of photoproducts. In addition the photoproduct ratios are intensity dependent; i.e., the ratios are different with the pulsed and CW laser irradiation.

The interpretation of the photoproduct ratios obtained from IRMPD of **2a** and **3b** is complicated by the small enthalpy difference between the two photoproduct channels, i.e., the 0.5 kcal/mol difference between CD_3O^- and CH_3O^- for **2a** and **2b** and the 0.05 kcal/mol difference between $CD_3CH_2O^-$ and $CH_3CH_2O^-$ for **3a** and **3b**. Although these energy differences are not large enough to cause total predominance of energetically favored photoproduct, the photoproduct ratios are skewed by this energetic preference. This preference is expected to be much less pronounced in the photodissociation of **3a** and **3b**, due to the smaller energetic difference between the two dissociation channels.

Another consideration in the infrared dissociation of the deuterated complexes is the possibility that the different complexes will have different photon absorption rates due to the small frequency changes induced by the deuteriums. For example, if the vibrational spectrum of **2a** is different from that of **2b**, their IR pumping rates could be different and the photoproduct ratios affected by this difference. This effect is expected to be small, however, compared to the energetic differences in the photodissociation channels.

The results obtained for each proton-transfer system and the implications of the observed photoproduct ratios are discussed below.

$^{12}CH_3OHO^{13}CH_3$. The putative proton-bound intermediate in the reaction of methoxide with methanol-^{13}C was synthesized in two different ways, as discussed above. Pulsed laser photolysis of the complex arising from the reaction of $^{12}CH_3O^-$ with $HCOO^{13}CH_3$ (**1a**) yielded a predominance of $^{13}CH_3O^-$ as the photoproduct. This preference is not a consequence of the thermodynamics, since the two alkoxide ions are equivalent in energy. More importantly, in addition, pulsed laser photolysis of the complex arising from the reaction of $^{13}CH_3O^-$ with $HCOO^{12}CH_3$ (**1b**) yielded a predominance of the other alkoxide ion, $^{12}CH_3O^-$. Thus the product dependence is not some artifact of peculiar absorption. This differentiation indicates that the two complexes must be distinct from each other. In addition, this suggests that the fast photon absorption rate of the complex, arising from the high intensity of the pulsed laser, competes favorably with the complex interconversion, so that the dissociation threshold is reached before proton equilibration is complete. As discussed above, this situation is expected to arise only if a substantial barrier to interconversion exists between the two complexes.

The dependence of the photoproduct ratio on the photon absorption rate is clearly seen from the results of CW laser photolysis: photodissociation of **1a** and **1b** yields equal amounts of the two alkoxide photoproducts. In this case, the low-intensity irradiation of the CW laser gives rise to a correspondingly low photon absorption rate. Interconversion and proton transfer then compete successfully with photon absorption, and proton equilibrium occurs before the dissociation threshold is reached.

$CD_3OHOCH_3^-$. The intermediates in the reaction between methoxide and methanol-d_3 were also synthesized in two different ways: from deuterated methoxide and methyl formate (**2a**) and from methoxide and deuterated methyl formate (**2b**). These intermediates are similar to the carbon-13-labeled complexes discussed above. An additional consideration in the deuterated complexes, however, is the 0.5 kcal/mol acidity difference[5,19] between CH_3OH and CD_3OH. This acidity difference indicates that the methoxide dissociation channel will be thermodynamically favored over the deuterated methoxide channel, and also that a complex composed of methoxide and deuterated methanol will be favored over one of deuterated methoxide and methanol.

Pulsed laser photolysis yields predominantly CH_3O^- in both complexes, along with some CD_3O^-. For a thermal distribution of alkoxide–alcohol complexes at 350 K, the estimated temperature of the ICR cell,[28] the equilibrium methoxide/deuterated methoxide ratio is ca. 2.0. As in the ^{13}C-labeled complexes discussed above, the photoproduct ratios obtained from pulsed laser irradiation are different in **2a** and **2b**. In **2a**, the unlabeled/labeled photoproduct ratio is larger than the prediction based on a thermal distribution,

(24) (a) Jasinski, J.; Rosenfeld, R. N.; Meyer, F. K.; Brauman, J. I. *J. Am. Chem. Soc.* **1982**, *104*, 652. (b) Tumas, W.; Foster, R. F.; Pellerite, M. J.; Brauman, J. I. *J. Am. Chem. Soc.* **1987**, *109*, 961.

(25) Moylan, C. R.; Brauman, J. I. *Int. J. Chem. Kinet.* **1986**, *18*, 379.

(26) Lias, S. G.; Bartmess, J. E.; Liebman, J. F.; Holmes, J. L.; Levin, R. D.; Mallard, W. G. *J. Phys. Chem. Ref. Data* **1988**, *17*.

(27) Bomse, D. S.; Beauchamp, J. L. *J. Am. Chem. Soc.* **1981**, *103*, 3252.

(28) Han, C.-C. Ph.D. Thesis, Stanford University, 1987.

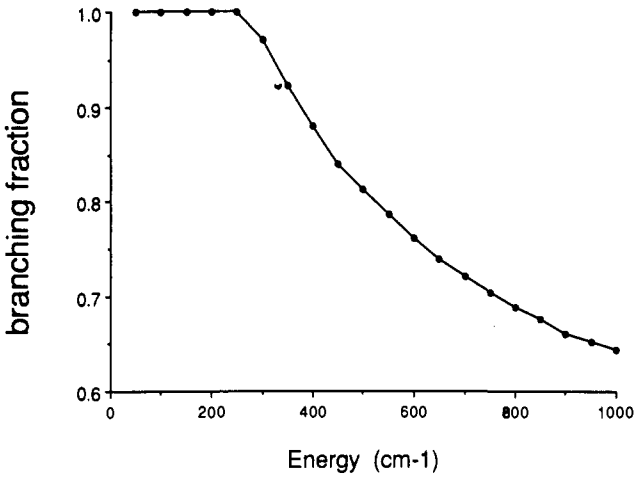

Figure 5. The microcanonical branching fractions, $\phi(E)$, for the dissociation of vibrationally excited $CD_3OHOCH_3^-$, defined as the yield of undeuterated methoxide over the total photoproduct yield, calculated using eqs 7–10 in the text. Below 200 cm^{-1}, only the threshold for CH_3O^- has been crossed, and therefore the branching fraction is 1.

and in **2b** the ratio is slightly smaller. This differentiation suggests that the two complexes are distinct from each other. The photoproduct ratios are influenced not only by the thermodynamics of the dissociation channels but also by the original structure of the alkoxide–alcohol complex.

Low-intensity irradiation of both **2a** and **2b** with the CW laser yields an average product ratio of 4.8/1 undeuterated to deuterated methoxide, a sizable secondary isotope effect. The plausibility of this observed photoproduct ratio can be checked using statistical theory to calculate a predicted photoproduct ratio.[29] This predicted ratio depends on the relative rates of dissociation out through the deuterated (yielding CD_3O^-) and undeuterated (yielding CH_3O^-) channels, the energy distribution of the vibrationally excited complexes, and the difference in energy between the channels.

Using RRKM theory,[30] the unimolecular dissociation rate of the lowest energy channel (CH_3O^- + CD_3OH) at a particular energy, $k(E)$, can be calculated by eq 7. In this equation σ is the reaction path degeneracy, $N(E)$ is the density of internal rotational and vibrational states of the stable alkoxide–alcohol complex at energy E, E_0 is the threshold energy required for dissociation, $G(E - E_0)$ is the sum of internal states for the dissociation transition state at energy E, and h is Planck's constant. The structure of

$$k(E) = \sigma G(E - E_0)/hN(E) \quad (7)$$

the transition state was modeled as a loose complex of methoxide and deuterated methoxide. The frequencies for both the reactant complex and the transition state were approximated by those for the undeuterated methoxide and methanol.[31] They are shown in Table II, along with the moments of inertia.

The dissociation rate of the higher energy channel (CD_3O^- + CH_3OH) at energy E, $k'(E)$, can be described by eq 8, where E_0' equals E_0 plus the difference in energy between the two channels, ΔE_0, i.e., 0.5 kcal/mol.

$$k'(E) = \sigma G(E - E_0')/hN(E) \quad (8)$$

Assuming that the sums of states of the two dissociation transition states, $CD_3O^-\cdots HOCH_3$ and $CH_3O^-\cdots HOCD_3$, are similar for a given small energy above each transition state and that the difference in energy between the two dissociation channels, ΔE_0, is approximately the difference in energy between the two reactant complexes, $CD_3O^-\cdot HOCH_3$ and $CH_3O^-\cdot HOCD_3$, then $k'(E)$ can be approximated by $k(E - \Delta E_0)$. The photoproduct branching ratio at a particular energy, $\phi(E)$, can be defined by eq 9. The calculated microcanonical branching ratios versus

$$\phi(E) = \frac{k(E)}{k(E) + k(E - \Delta E_0)} \quad (9)$$

energy are shown in Figure 5. They range from 1, below the threshold for CD_3O^- dissociation, to 0.62, 1000 cm^{-1} above the threshold for CH_3O^- dissociation.

To obtain the canonical branching ratio, ϕ, the microcanonical branching ratios, the $\phi(E)$'s, must be integrated over the energy distribution of the vibrationally excited molecules, $P(E)$, as shown in eq 10, where x is an estimated upper limit for the energetic distribution. Owing to the slow nature of the CW laser irradiation

$$\phi = \int_{E_0}^{x} \phi(E)P(E)\,dE \quad (10)$$

(photon absorption rate $\approx 10^2$ s^{-1}), as soon as a molecule attains the threshold energy, E_0, it is assumed to dissociate. Since the photon absorption process is integral ($h\nu \approx 3$ kcal/mol), absorption of the "final" photon will produce a distribution of molecules whose energies range from the threshold, E_0, to 3 kcal/mol above threshold. Thus, the upper integration limit in eq 10, x, is taken to be 3 kcal/mol. Two different approximations for $P(E)$ were used: a uniform distribution of energy and an exponential distribution of energy, $e^{-E/kT}$, where k is the Boltzmann constant and T was taken to be 350 K.

Table III. Comparison of Theoretical and Experimental Photoproduct Branching for $CD_3OHOCH_3^-$

	theor[a]		
	$P(E) = 1$	$P(E) = e^{-E/kT}$[b]	exptl
ϕ	0.82	0.95	0.83
CH_3O^-/CD_3O^-	4.6/1	19/1	4.8/1

[a] Calculated using eqs 7–10. [b] k is the Boltzmann constant. T was taken to be 350 K.

As can be seen in Table III, the uniform energetic distribution, which gives each $\phi(E)$ equal weight, resulted in a predicted overall branching fraction of 0.82, corresponding to an undeuterated to deuterated methoxide ratio of 4.6/1. The exponential energetic distribution, which weights the lower energy branching fractions more highly, resulted in a branching fraction of 0.95, or a photoproduct ratio of 19/1. The experimental branching fraction of 0.83 (photoproduct ratio of 4.8/1) lies much closer to the uniform distribution. This suggests that the distribution of ions excited to energies just below the threshold is relatively uniform.

$CH_3CH_2OHOCH_2CD_3^-$. The intermediates in the reaction between ethoxide and ethanol-d_3 were also synthesized in two ways. Complex **3a**, formed by reaction of $CD_3CH_2O^-$ with $HCOOCH_2CH_3$, yielded an unlabeled/labeled ethoxide ratio of 2.5/1 upon pulsed laser irradiation, while **3b**, formed by reaction of $CH_3CH_2O^-$ with $HCOOCH_2CD_3$, yielded a photoproduct ratio of 1.1/1. This behavior, which is consistent with the alkoxide–alcohol complexes described above, implies that the two ethoxide–ethanol complexes are not identical; they retain a structural memory of the method of formation.

The proton-transfer reaction of $CH_3CH_2O^-$ with CD_3CH_2OH is estimated to be 0.05 kcal/mol endothermic, and thus, one might expect the reaction intermediates (**3a** and **3b**) to display photochemical behavior similar to that of the intermediates in the reaction of CH_3O^- with CD_3OH (**2a** and **2b**). This behavior is observed, although the extent of the energetic preference for the unlabeled alkoxide is attenuated relative to the deuterated methanol system. Pulsed laser irradiation of both **3a** and **3b** favors the thermodynamic product, $CH_3CH_2O^-$, although the ratios of unlabeled to labeled alkoxide are smaller than those obtained for **2a** and **2b**.

Irradiation of both **3a** and **3b** with the CW laser yields approximately twice as much $CH_3CH_2O^-$ as $CD_3CH_2O^-$, corresponding to a branching fraction of 0.70. As in the case of the

(29) Hase, W. L.; Bunker, D. L. *QCPE* No. 234, Indiana University.
(30) (a) Forst, W. *Theory of Unimolecular Reactions*; Academic Press: New York, 1973. (b) Robinson, P. J.; Holbrook, K. A. *Unimolecular Reactions*; Interscience: London, 1972.
(31) Shimanouchi, T. *Tables of Molecular Vibrational Frequencies*; National Standard Reference Data Series; NBS: Washington, DC, 1972; Consolidated Vol. 1.

Table IV. Input Parameters for RRKM Calculation of Ethoxide + Ethanol

reactant complex: $(CH_3CH_2O^-\cdot HOCH_2CH_3)$			orbiting transition state: $(CH_3CH_2O^-\cdots HOCH_2CH_3)$		
ν_i (cm^{-1})[a]		I_i (amu·Å), σ_i[b]	ν_i (cm^{-1})[a,c]		I_i (amu·Å), σ_i[b]
3676	1225		3676	1225	
2989	1200	28.73,[c] 1 (1)	2989	1200	34.90,[c] 1 (1)
2989	1134		2989	1134	7.88, 1 (1)
2949	1089		2949	1089	68.98, 1 (2)
2949	1062		2949	1062	55.49, 1 (2)
2943	1045		2943	1045	
2904	1033		2904	1033	
2900	1024		2900	1024	
2225	925		2225	925	
2225	925		2225	925	
2115	885		2115	885	
1490	801		1490	801	
1490	756		1490	756	
1452	668		1452	668	
1452	419		1452	419	
1415	370		1415	370	
1394	300		1394	243	
1385	300		1385	201	
1339	300		1339	170	
1251	300		1251		
243					
201					
200					
200					
170					
$I_{reactant\ complex}$ = 564.36 amu·Å			$I_{transition\ state}$ = 1262.41 amu·Å		

[a] Reference 32. Frequencies for EtO^- were taken from those of EtOH. [b] Degeneracy is in parentheses. [c] External rotation about the internuclear axis treated as an internal rotation able to exchange energy with other modes.

Table V. Comparison of Theoretical and Experimental Photoproduct Branching Fractions for $CD_3CH_2OHOCH_2CH_3^-$

	theor[a]		
	$P(E) = 1$	$P(E) = e^{-E/kT}$[b]	exptl
ϕ	0.57	0.65	0.70
$CH_3CH_2O^-/CD_3CH_2O^-$	1.3/1	1.9/1	2.3/1

[a] Calculated using eqs 7–10. [b] k is the Boltzmann constant. T was taken to be 350 K.

deuterated methanol system, the magnitude of the observed isotope effect is quite large, considering the energy difference between the two channels. Again, to confirm the plausibility of these large isotope effects, the microcanonical branching fractions, $\phi(E)$, were calculated as described above, using eqs 7–9. In this system, the difference in energy between the two dissociation channels ($CH_3CH_2O^-$ + CD_3CH_2OH and $CD_3CH_2O^-$ + CH_3CH_2OH), ΔE_0, is an order of magnitude smaller than the methanol system (as calculated above). The vibrational frequencies of the reactant complex and the transition state, along with the appropriate moments of inertia, given in Table IV, are approximated by those of undeuterated ethoxide and ethanol.[32] The microcanonical branching fractions are shown in Figure 6, as a function of energy of the threshold, E_0. They range from 1.0, at E_0, to 0.52, 1000 cm^{-1} above E_0.

The canonical branching fraction, ϕ, was calculated by eq 10, again taking 3 kcal/mol as the upper limit of integration, x, and using both a uniform and an exponential ($e^{-E/kT}$, where k is the Boltzmann constant and T is taken to be 350 K) distribution of energy for $P(E)$. The predicted branching fraction obtained for both distributions, as well as the experimental branching fraction, is shown in Table V. The uniform distribution resulted in a predicted branching fraction of 0.57, corresponding to an undeuterated to deuterated ethoxide ratio of 1.3/1. The exponential distribution resulted in a predicted branching fraction of 0.65, corresponding to a 1.9/1 photoproduct ratio. The experimentally observed branching fraction, 0.70 (2.3/1 photoproduct ratio), is closer to the result predicted from the exponential distribution; however, the uncertainty in the experimental value, as well as in $\Delta E°$, the estimated acidity difference between deuterated and

(32) (a) Perchard, J. P.; Josien, M. L. *J. Chim. Phys.* **1968**, *65*, 1834, 1856. (b) Barnes, A. J.; Hallam, H. E. *Trans. Faraday Soc.* **1970**, *66*, 1932.

Table VI. Experimental Photoproduct Ratios Obtained for Alkoxide–Alcohol Decompositions

A. $^{13}CH_3O^- + HCOO^{12}CH_3$		
Pulsed Laser ($^{12}CH_3O^-/^{13}CH_3O^-$)		
1.59	1.70	1.50
1.26	1.69	1.29
1.53	1.64	1.24
1.71	1.51	1.25
1.48	1.49	1.31
1.52	1.48	1.31
		1.32
CW Laser ($^{12}CH_3O^-/^{13}CH_3O^-$)		
1.0	0.9	1.1
1.0	1.0	1.0
	1.1	
B. $^{12}CH_3O^- + HCOO^{13}CH_3$		
Pulsed Laser ($^{12}CH_3O^-/^{13}CH_3O^-$)		
0.67	0.83	0.71
0.67	0.88	0.85
0.50	0.83	0.73
0.64	0.83	0.71
0.62	0.80	0.72
0.68	0.81	0.83
0.71	0.70	0.74
0.81	0.71	0.71
0.83	0.65	0.79
CW Laser ($^{12}CH_3O^-/^{13}CH_3O^-$)		
1.0	1.1	0.9
1.0	1.0	0.9
C. $CD_3O^- + HCOOCH_3$		
Pulsed Laser (CH_3O^-/CD_3O^-)		
4.08	5.17	3.07
4.87		5.27
CW Laser (CH_3O^-/CD_3O^-)		
4.95	5.47	5.36
4.67		4.93
D. $CH_3O^- + HCOOCD_3$		
Pulsed Laser (CH_3O^-/CD_3O^-)		
2.02	2.35	2.02
2.07	2.07	1.90
2.03	2.02	1.80
CW Laser (CH_3O^-/CD_3O^-)		
4.98	4.21	3.98
5.08	3.54	1.98
7.90	3.98	3.26
3.62	1.93	2.74
	3.33	
E. $CD_3CH_2O^- + HCOOCH_2CH_3$		
Pulsed Laser ($CH_3CH_2O^-/CD_3CH_2O^-$)		
2.2	2.7	2.8
2.3	2.5	2.9
CW Laser ($CH_3CH_2O^-/CD_3CH_2O^-$)		
2.2	2.8	2.9
2.3		2.9
F. $CH_3CH_2O^- + HCOOCH_2CD_3$		
Pulsed Laser ($CH_3CH_2O^-/CD_3CH_2O^-$)		
1.01	0.87	1.21
0.96	0.91	1.18
1.03		1.20
CW Laser ($CH_3CH_2O^-/CD_3CH_2O^-$)		
2.76	2.08	1.85
2.29	1.95	1.96
2.13		1.92

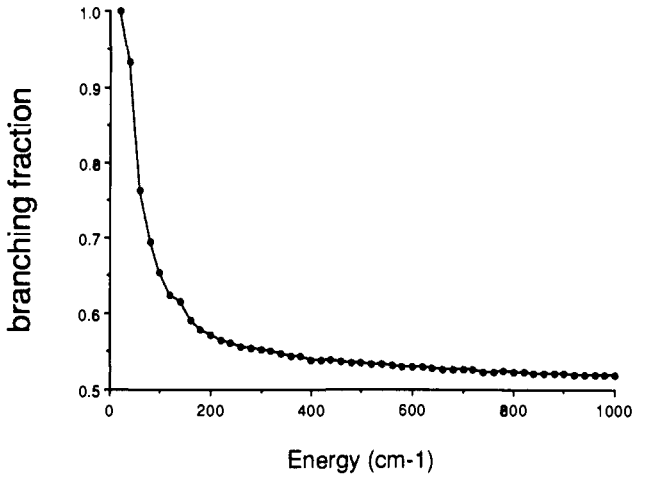

Figure 6. The microcanonical branching fractions, $\phi(E)$, for the dissociation of vibrationally excited $CD_3CH_2OHOCH_2CH_3^-$, defined as the yield of undeuterated ethoxide over the total photoproduct yield, calculated using eqs 7–10 in the text. Below 20 cm^{-1}, only the threshold for $CH_3CH_2O^-$ has been crossed, and therefore the branching fraction is 1.

undeuterated ethanol, makes it difficult to differentiate between the branching fractions predicted by the uniform and exponential distributions.

Conclusions

Alkoxide–alcohol complexes for three different proton-transfer reaction systems, i.e., $^{12}CH_3OHO^{13}CH_3^-$, $CH_3OHOCD_3^-$, and $CH_3CH_2OHOCH_2CD_3^-$, were synthesized in an asymmetric manner using isotopic labeling. For each system, IRMPD of the complex produced from RO^- + HCOOR′ gave photoproduct results different from those of the complex produced from $R'O^-$ + HCOOR. In the case of the essentially thermoneutral $^{12}CH_3OHO^{13}CH_3^-$ system, the observed ratios were roughly the inverse of each other, i.e., $^{12}CH_3O^-/^{13}CH_3O^- = 1.46$ for one complex and 0.73 for the other. The photoproduct ratios for the deuterated methanol and ethanol systems were skewed by the small energetic preference for the unlabeled alkoxide. Despite this thermodynamic effect, the asymmetric complexes yielded different photoproduct ratios.

These asymmetric photoproduct ratios indicate that alkoxide–alcohol complexes *formed in this manner* retain some memory of their method of synthesis; the distinction between the alkoxide and the alcohol is not lost by rapid proton transfer. This striking result, which suggests the presence of some kind of bottleneck, may or may not be related to the slow observed proton-transfer kinetics.[6] A large enthalpic proton-transfer barrier on the minimum energy path is precluded, however, by the results of quantum mechanical calculations which suggest a near barrierless potential surface.

Additional information about these alcohol–alkoxide complexes is found in the electron photodetachment spectroscopy of the methoxide–methanol complex formed by the Riveros reaction, reported by us several years ago.[33] The binding energy of the methoxide–methanol complex extracted from the photodetachment spectrum was 19 kcal/mol, 10 kcal/mol less than that reported by Paul and Kebarle[9a] and Meot-Ner and Sieck.[9b,c] This discrepancy, which would be slightly less if the neutral dimer were more strongly bound than we had assumed, is not fully understood. In conjunction with the results reported in this paper, however, it suggests that alkoxide–alcohol complexes synthesized by the Riveros reaction do not behave like the stable, hydrogen-bonded reaction intermediates on the minimum energy proton-transfer reaction potential surface.

A possible rationalization of these results is that the Riveros reaction produces an intermediate which is a secondary local minimum on the reaction surface and whose geometry is not that of the stable, hydrogen-bonded complex, $ROH\cdot^-OR$. Such an intermediate would have to be relatively nonreactive to proton transfer, as indicated by the IRMPD results, and would have to be bound by ca. 20 kcal/mol, as suggested by the electron photodetachment study. A binding energy of 20 kcal/mol is more consistent with a strong ion–dipole bond rather than a hydrogen bond. A possible candidate would be a structure resembling the S_N2 reaction intermediate, for which some barrier to rearrangement might well be expected. Our preliminary quantum calculations show that such minima can exist, but that barriers to rearrangement are small. Another possibility is a complex in which the alkoxide is hydrogen bonded to the protons on the α-carbon of the alcohol. A structure of this nature has been reported to be a minimum in the calculation of the $F^- + CH_3F$ reaction surface.[34] More extensive quantum calculations on the methanol–methoxide surface should be helpful in elucidating these issues.

Acknowledgment. We are grateful to the National Science Foundation for support of this work. S.B. gratefully acknowledges graduate fellowship support from the Evelyn McBain Fund. We also thank Dr. Kieran F. Lim for many stimulating discussions.

Appendix

The averages of the photoproduct ratios listed in Table VI are not always the same as the final photoproduct ratios, reported in Table I. This is because the average ratios for each day were obtained *before* the overall average. This method was deemed to be most accurate, because the day to day fluctuations in the photoproduct ratios were greater than the fluctuations on any given day.

Registry No. D_2, 7782-39-0; methoxide, 3315-60-4; methanol, 67-56-1; ethoxide, 16331-64-9; ethanol, 64-17-5; methyl formate, 107-31-3; ethyl formate, 109-94-4.

(33) Moylan, C. R.; Dodd, J. A.; Han, C.-C.; Brauman, J. I. *J. Chem. Phys.* **1987**, *86*, 5350.
(34) Schlegel, H. B.; Mislow, K.; Bernardi, F.; Bottoni, A. *Theoret. Chem. Acta*, **1977**, *44*, 245.